CON CERTO

Deliverable D5.1 – Synthesis report on carbon cycle processes developments

Lead Beneficiary: BSC

Authors:

Etienne Tourigny, Souhail Boussetta, Anna Agusti-Panareda, Timothee Corchia, Patricia de Rosnay, Sebastien Garrigues, Giulia Mengoli, Daniele Peano, Manuela Balzarolo, Carlo Camporeale, Narender Reddy Kangari.

30/06/2026

Funded by the European Union

Prepared under contract from the European Commission

Grant agreement No. 101185000

Project acronym:	CONCERTO
Project full title:	Improved CarbOn cycle represeNtation through multi-sCale models and Earth obseRvation for Terrestrial ecOsystems
Start of the project:	January 2025
Duration:	48 months
Project coordinator:	Manuela Balzarolo
Deliverable title:	Synthesis report on carbon cycle processes developments
Deliverable n°:	D5.1
Nature of the deliverable:	Report
Dissemination level:	Public
WP responsible:	WP5
Lead beneficiary:	BSC
Citation:	Tourigny, E., Boussetta, S., Agusti-Panareda, A., de Rosnay, P., Garrigues, S., Mengoli, G., Peano, D., Balzarolo, Carlo Camporeale, M., Kangari, N. R. (2026). ***Synthesis report on carbon cycle processes developments.*** Deliverable D5.1. Horizon Europe CONCERTO project, Grant Agreement No 101185000.
Due date of deliverable:	Month n° 18
Actual submission date:	Month n° 18
Deliverable status:	Submitted

Version	Status	Date	Author(s)/Reviewer
1.0	Draft	10 June 2026	BSC, ECMWF, CMCC, UReading

1.1	Reviews	29 June 2026	Josep Peñuelas, Jennifer Adams Sandy Harrison
1.3	Revised version	29 June 2026	BSC
2.0	Final	30 June	Project management office

Contents

1. Preface

The activities performed within the fifth Working Package (WP5) of the CONCERTO project aim to improve the representation of the main land carbon processes within the land component (LSM) of state-of-the-art Earth system models (ESMs). In particular, the WP5 leverages ongoing work within a related project, LEMONTREE, and leverages data from the CONCERTO Working Packages (WP1 and WP2) as novel boundary conditions for LSMs and references for model developments.

Additionally, the developments achieved in the third and fourth WPs (WP3 and WP4) are complementary to the activities performed in WP5. Finally, the WP5 developments provide the basis for planned simulations of the sixth Working Package (WP6).

In particular, this deliverable describes the status of the developments within the first WP5 task, focusing on the development of the LSMs' representation of carbon cycle processes.

Note that the outcomes presented in this deliverable are to be considered as preliminary results, since the complete task results will be reached in month 36 and summarised in deliverable D5.2. The status of each activity within the first task of WP5 is listed in Table 1.

Table 1: Summary of the status of development for each activity of the first task of WP5. Complete stands for developments that reached their conclusion; Ongoing stands for developments started within the initial 18 months of the project and will continue in the next 18-month period; Planned stands for developments in their preliminary stages and that will be developed during the next 18 months.

Activity	Status
Lateral Carbon dynamics	Planned
Prognostic LAI	Complete
P model implementation in LSMs	Ongoing
Implementation of ecLand in EC-Earth	Ongoing
Improve Ecosystem Respiration in ecLand	Planned

2. Summary

The present deliverable provides a brief summary of the ongoing development performed within the first task of CONCERTO's fifth Working Package (WP5). The principal aim of these developments is to improve the representation of the carbon cycle within a set of state-of-the-art land surface models (LSMs). In particular, this task aims at addressing processes that are missing in state-of-the-art LSMs, such as the lateral carbon dynamics in the Community Land Model (CLM), improving processes representation, such as the introduction of prognostic Leaf Area Index (LAI) computation and ecosystem respiration in ecLand, harmonising processes, such as the implementation of the P model approach for simulating vegetation photosynthesis within various LSMs, and the implementation of new LSMs in an Earth System Model (ESM) framework, as planned for ecLand within EC-Earth4.

LSMs are used to estimate the land portion of the global carbon budget. However, some processes that influence the fluxes of carbon from land to ocean, i.e. through rivers, and atmosphere, i.e. through outgassing, are not incorporated in state-of-the-art LSMs. One of these missing processes is the lateral carbon transport. CONCERTO aims to include this process in CLM to estimate uncertainties in the global carbon budget estimates derived from its absence. A preliminary literature review and development plan have been established within the first 18 months of the project.

LAI describes the amount of canopy leaves in the LSM simulations. The LAI depends on many factors, and various schemes are used to simulate it. As part of CONCERTO, a prognostic LAI is implemented within the ecLand model using a simple growth model based on the daily carbon balance at the leaf level. This addition increases the ability of ecLand to estimate the impact of boundary conditions on the carbon cycle variability.

Photosynthesis is the principal process for simulating land-atmosphere carbon fluxes. Consequently, most of the uncertainties between LSMs in carbon cycle estimates may derive from differences in the scheme used to represent photosynthesis. For this reason, a common scheme for photosynthesis, namely the P model, is proposed and implemented in different LSMs within WP5 of CONCERTO. The status of P model implementation in each LSM is at a different stage, but all LSMs are producing a preliminary comparison between the standard configuration and the one with the P model at site level.

A preliminary implementation of the ecLand LSM within the EC-Earth4 ESM framework is ongoing and will allow an assessment of the performance of the carbon cycle representation in both land-only and coupled configurations.

3. List of Abbreviations

CLM – Community Land Model

EEO – Eco-Evolutionary Optimality

ESM – Earth System Model

GPP – Gross Primary Production

LAI – Leaf Area Index

LSM – Land Surface Model

PFT – Plant Functional Type

WP – Working Package

BATS – Biosphere-Atmosphere Transfer Scheme

4. Lateral Carbon dynamics

During the first 18 months, work on lateral carbon dynamics has focused on consolidating the process basis, observational assets and modelling concepts required for the future implementation of lateral carbon transport and riverine greenhouse-gas outgassing in CLM. This activity is aligned with T5.1, where CMCC and POLITO contribute to the implementation of soil carbon lateral dynamics and GHG outgassing from rivers in CLM, and anticipates the evaluation phase planned in T5.4 over Northern Italian Hydrographic Districts and selected European basins.

4.1. Status of developments

The following activities have been performed:

- Representation of transport and dispersion in complex river networks. Vendruscolo et al. (2025) developed an analytical framework for network-driven dispersion in directed transport networks, with applications to braided rivers. The framework identifies river-network topology, edge travel times and bifurcation partitioning as controlling factors of scalar transit-time distributions, and it can also account for decay processes. This provides a conceptual and mathematical basis for simplified routing formulations of laterally mobilised carbon and related material through multi-thread river corridors.

- Observation of carbon-relevant geomorphic and ecological features in river corridors. POLITO developed and tested an automated RGB-UAV and AI-based workflow for detecting large woody debris in the Tagliamento River (Han et al, 2026), one of the POLITO experimental sites identified for CONCERTO. These results support the construction of site-level datasets for parameterising and evaluating lateral carbon recruitment and transport processes.
- Characterisation of coastal and transitional ecosystems relevant to the downstream fate of laterally transported carbon at the San Rossore–Migliarino–Massaciuccoli Regional Park, another POLITO experimental site and development of a physically based stochastic framework for coastal dune vegetation dynamics under random wind and runup disturbances (Camporeale & Latella, 2025). The model was validated against satellite imagery and high-resolution topographic data, and it quantifies how dune morphology, forcing variability and disturbance thresholds affect vegetation stability. Although developed for coastal dunes, this approach contributes to CONCERTO by strengthening the process-based representation of vegetation response to stochastic hydro-geomorphic forcing in carbon-relevant transitional environments.

4.2. Future developments

We intend to extend the dimensionless framework developed by Bertagni et al. (2024) to investigate the global controls on fluvial inorganic carbon partitioning. Specifically, it quantifies the spatial and temporal variability of the dimensionless number Π_τ, which determines the fate of out-of-equilibrium inorganic carbon between atmospheric CO_2 evasion and downstream transport. Using global hydrological and geomorphological datasets, the study will assess the influence of stream order, climate, and hydrological variability on Π_τ across river networks worldwide. The results will reveal large-scale patterns in the role of rivers as connectors between terrestrial, atmospheric, and oceanic carbon pools.

5. Prognostic LAI

5.1. Model implementation

ECMWF is developing a prognostic Leaf Area Index (LAI) module in its land surface model ecLand (Boussetta et al., 2021). The LAI is simulated with a simple growth model based on the daily carbon balance at the leaves level following Gibelin et al. (2006) and Calvet and Sousana (2001). The LAI is computed from the leaf biomass B derived from the net canopy assimilation A_{nI}. Growth is the result of carbon accumulation obtained from assimilation of atmospheric CO_2 and senescence related to the photosynthesis deficit due to environmental factors. LAI is obtained from the product of the green leaf biomass B with the Specific Leaf Area (SLA) which is a function of leaf nitrogen concentration dependent on vegetation types following:

$$LAI = B \cdot SLA = B \cdot e \cdot N_l + f \quad (1)$$

where N_L is the leaf Nitrogen concentration, and e, f are respectively the slope and intercept nitrogen plasticity parameters which vary by vegetation types (Table 2). For global scale applications and to reduce drifts caused by forcing errors, the computed biomass is updated by a relaxation formulation toward climatological biomass values B_C (based on climatological LAI); the final biomass value B_f follows:

$$B_f = r_B \cdot B + (1 - r_B) \cdot B_C \qquad (2)$$

where r_B is the relaxation coefficient.
The green leaf biomass B is obtained from the following differential equation:

$$dB = \frac{M_c}{P_c M_{CO_2}} A_{nI} dt - Bd(t/\tau) \quad (3)$$

P_c here is the proportion of carbon in the dry plant biomass, and M_c and M_{CO_2} are the molecular weights of carbon and CO_2 , respectively. The mortality increment term of equation (3) represents an exponential extinction of B characterised by a time-dependent effective life expectancy (expressed in units of days):

$$\tau(t) = \tau_M \frac{A_{nIm}(t)}{A_{n,max}} \qquad (4)$$

This development relies on having a simple allocation scheme for the total nonwoody aboveground biomass B_T which is considered as the sum of the leaf biomass B and the structural biomass B_s. In the nitrogen decline (N-decline) model, B_T is related to the leaf biomass B by the allometric equation following Calvet and Sousana (2001):

$$B_T = \left(\frac{B}{c}\right)^{1/(1-a)} \qquad (5)$$

where c and a are constant parameters ($c = 0.754$, $a = 0.38$).

The B-decline term is split into a mortality and a storage term (M_B and S_B , respectively):

$$Bd(t/\tau) = M_B + S_B \qquad (6)$$

In equation (3) when net assimilation exceeds the B-decline term a growing phase is happening with positive values of dB. In this case the plant N-decline model is triggered and the aboveground biomass B_T is derived from B using equation (5). While the structural biomass B_s is expressed as the difference between the total aboveground biomass B_T and the leaf biomass B. The mortality of the structural biomass M_{Bs} is then computed by:

$$M_{Bs} = B_s d(t/\tau_M) \qquad (7)$$

In addition, a loss of carbon is simulated through the structural biomass respiration with:

$$R_{Bs} = \eta_R B_S Q_{10}^{(T-25)/10} dt \qquad (8)$$

where dt is one day step, T the surface temperature (in °C), η_R a respiration coefficient of 1% of B_s per day, and $Q_{10} = 2$.

The storage S_B term is calculated as the residual of the structural biomass budget:

$$S_B = dB_s + M_{B_s} + R_{B_s} \qquad (9)$$

An alternative formulation of B-decline is used when the storage exceeds the mortality of active biomass M_B. B_T is recalculated assuming that there is no loss of leaf biomass outside the plant system, during the considered time step, $M_B = 0$ and dB_T is the difference between the daily net assimilation and the mortality and respiration losses of structural biomass following equations (5) and (6).

The leaf biomass B is derived from B_T using the N-decline equation, and B_s is the difference between the two terms, an updated value of S_B is then computed by equation (9). When db becomes negative, the vegetation is senescent and the N-decline equation is not valid anymore; In such configuration, the structural biomass reservoir B_s becomes independent from the leaf biomass reservoir B to which a nil value term is assigned and the mortality and respiration losses are applied to B_s using equations (5) and (6).

Table 2: Vegetation growth model parameters values as specified in ecLand model. The vegetation types follow a modified Biosphere-Atmosphere Transfer Scheme (BATS) classification

Type	*Vegetation type*	*e* [$m^2\ kg^{-1}\%^{-1}$]	*f* [$m^2 kg^{-1}$]	N_l [%]
1	Crops, mixed farming	3.79	9.84	1.3
2	Short grass	5.56	6.73	1.3
3	Evergreen needleleaf	4.85	-0.24	2.8
4	Deciduous needleleaf	4.85	-0.24	2.8
5	Deciduous broadleaf	4.83	2.53	2.0
6	Evergreen broadleaf	4.83	2.53	2.5
7	Tall grass	7.68	-4.33	1.3
8	Desert	-	-	-
9	Tundra	5.56	6.73	1.3
10	Irrigated crops	3.79	9.84	1.3
11	Semidesert	5.56	6.73	1.3
12	Ice caps and glaciers	-	-	-
13	Bogs and marshes	5.56	6.73	1.3
14	Inland water	-	-	-
15	Ocean	-	-	-
16	Evergreen shrubs	7.68	-4.33	1.3
17	Deciduous shrubs	5.56	6.73	1.3
18	Mixed forest- Wood	4.85	-0.24	2.8
19	Interrupted forest	4.85	-0.24	2.8
20	Water -land mixtures	5.56	6.73	1.3

5.2. Status of developments

The prognostic LAI module is now integrated in ecLand (Cycle 50R1.0). Initial testing showed a general behaviour of delayed onset of the model LAI. With the implementation of the relaxation toward climatology, the model is then run on several FLUXNET sites spanning different plant functional types (PFT), it showed substantial improvement over the original formulation, especially reducing the onset delay, compared with the CONFESS based LAI climatology and still preserving the inherent inter-annual variability (Figure1).

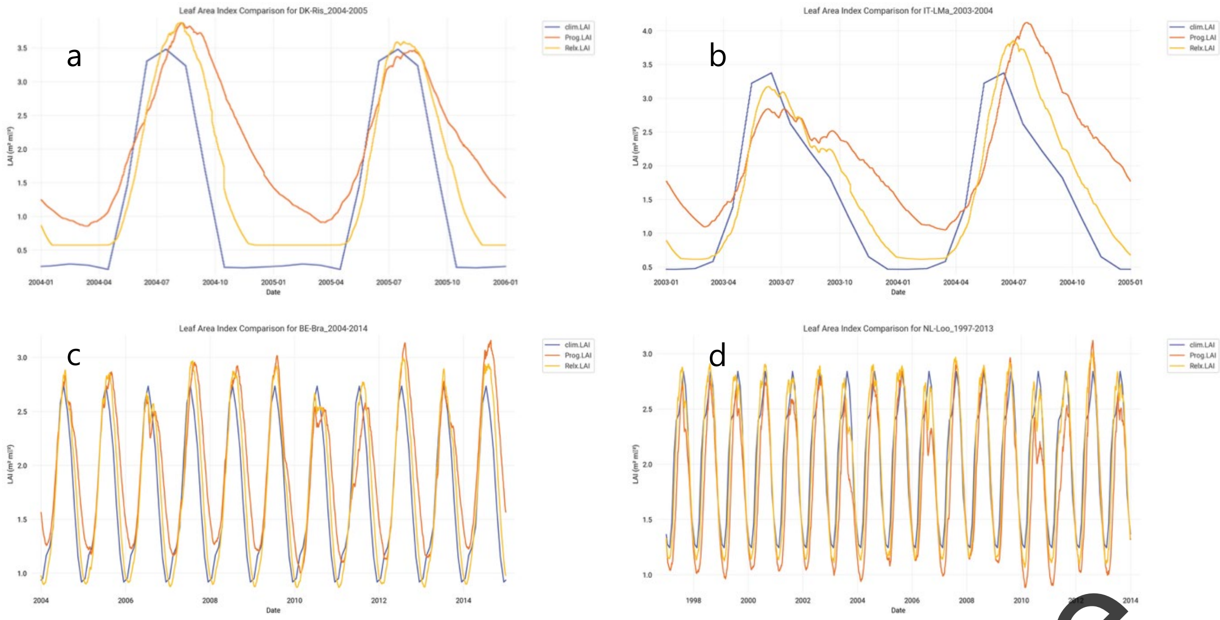

Figure 1: Simulated LAI from the original formulation (red), and using the relaxation formulation (orange) compared with the CONFESS LAI climatology Blue, (2010-2019) over different FLUXNET sites: (a) DK-Ris (Crop), (b) IT-LMa (Grass), (c) BE-Bra (Mixed Forest), (d) NL-Loo (ENF)

The LAI module was further implemented in ecLand in 2D mode allowing global simulations driven by ERA5 atmospheric forcing. Figure 2 shows the global LAI difference for JJA between years 2018 and 2017 from observation-based CONFESS data and simulated with ecLand. The global LAI differences between observed and simulated fields show similar patterns especially the drought area over Europe. These results will be further evaluated in task T5.4 and to further explore the model performance under extreme events.

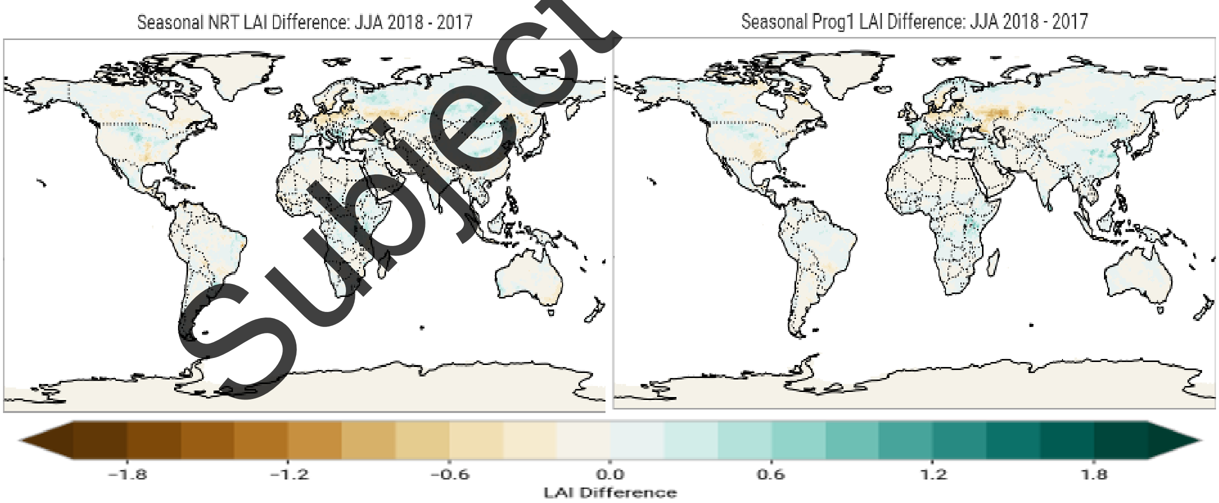

Figure 2: LAI differences for JJA 2018-2017: from the Near Real Time (NRT) Observation-based CONFESS data (left), and simulated by ecLand (right).

5.3. Future developments

The prognostic LAI implementation in ecLand is achieved, and its detailed evaluation will be performed in task T5.4. However, further improvements are planned under task T5.3 where model parameters will be further optimised to improve water, energy and CO2 fluxes.

6. P model implementation

The P model is based on eco-evolutionary optimality (EEO) theory (Wang et al. 2017; Stocker et al 2020; Cai and Prentice 2020; Mengoli et al. 2022) and simulates the gross primary production (GPP). It requires only a few meteorological and satellite derived data products, and a small number of parameters independently prescribed. The model incorporates two EEO-hypotheses (Maire et al. 2012; Prentice et al. 2014), which express the acclimation of plant photosynthetic capacities and stomatal behavior to the environmental variations. These lead key photosynthetic parameters to vary continuously and adjust to environmental changes according to general rules. As a consequence, the model is Plant Functional Type (PFT)-independent (except for the distinction between C_3 and C_4) and applicable in different biomes and climates with the same set of equations without having to change parameters between types of vegetation. Many current Land Surface Models (LSMs) represent only the instantaneous response of photosynthesis to environmental conditions, while modern versions represent also the acclimated response, but yet, using approaches that are highly dependent on fixed PFT-dependent parameters, with a tendency to parametrisation and an increase in model complexity (Fisher & Koven, 2020), which does not always lead to an increase in model accuracy/performances. Our aim is to apply the EEO theory (P model) to model photosynthesis in LSMs and assess whether this leads to improved simulations and future projections, and to a reduction in LSMs uncertainty and variability. The original P model (Wang et al. 2017; Stocker et al. 2020) implicitly predicts the plant adaptation and acclimation over timescales of days to weeks, and is designed to simulate GPP at weekly to monthly time steps. In this project, we use the sub-daily P model (Mengoli et al. 2022), which explicitly differentiates between the instantaneous and acclimated responses of key photosynthetic traits, to simulate GPP at half-hourly timesteps, as required for LSMs. The devised approach, designed for the P model implementation into LSMs, is a simple way to include acclimation within a land-surface framework, without having to store information on past conditions, which would be computationally costly.

6.1. Status of developments

To facilitate comparison across the different models, an implementation protocol for evaluating EEO components in LSMs has been designed. The protocol includes a basic minimum set of 10 flux sites and flux data source both for running and evaluating models. For each site, weeks and seasonal common periods have been selected based on the good quality and coverage of data to conduct the model intercomparison. The application of this protocol will be part of the evaluation task 5.4 and new PLUMBER2 flux sites will be included in the future analysis.

6.1.1. CLM implementation

The sub-daily P model (Mengoli et al. 2022) has been implemented offline to evaluate the impact of EEO-based photosynthesis, independently of feedback associated with prognostic carbon-water-energy coupling, within the CMCC community land model CLM (v5).

The implementation work covered the following tasks:

- Translation of the original P model code from Python to Fortran (CLM is coded in Fortran).
- Development of a modular implementation strategy to allow independent activation or deactivation of sub-daily P model components and facilitate process-level evaluation within the CLM framework.
- Implementation of the sub-daily P model acclimation scheme within the CLM framework, followed by checking the implementation results against the original standalone sub-daily P model.

The sub-daily P model integrated into CLM produces the same results both for its intermediate variables and for the final output (GPP, results not shown), when compared to the standalone P model results. So far, only the C3 schema of the sub-daily P model has been implemented and tested in CLM.

A preliminary evaluation of CLM and the sub-daily P model at 8 FLUXNET sites, highlighted some issues related to the simulated LAI from CLM and its potential impact on the final GPP. Thus, an evaluation of the standard CLM photosynthesis scheme and the standalone EEO-based P model at some sites was performed, using the same quality-controlled and gap-filled meteorological forcings from the PLUMBER2 dataset (Ukkola et al., 2022) and two different LAI sources: satellite-observed LAI from MODIS, one of the global satellite product available within PLUMBER2, and simulated LAI from CLM. This initial experiment was conducted using an offline configuration for CLM and the water stress function of CLMv4.5, which accounts for the soil moisture limitation to GPP. The stress function was applied only to the GPP of CLM and not to the P model's one. That is why only well-watered sites are shown here.

Figure 3 compares the standard photosynthesis scheme in CLM with the EEO-based photosynthesis scheme (P model), together with site observations, using the same forcing data. Overall, the sub-daily P model performs better than CLM at these three well-watered sites.

As illustrated in Figure 3 and Figure 4, the agreement between simulated and observed GPP decreases when the sub-daily P model is forced with CLM-simulated LAI instead of observed LAI. This effect is less evident at the tropical evergreen forest site (GF-Guy), but becomes more pronounced at sites with stronger seasonality (i.e. DE-Gri and DK-Sor), where the differences between observed and simulated LAI are much larger (Figure 4). Overall, the difference in GPP between simulations forced with simulated versus observed LAI is larger for the sub-daily P model than for CLM. This highlights a stronger dependency on LAI in the P model compared to the CLM scheme.

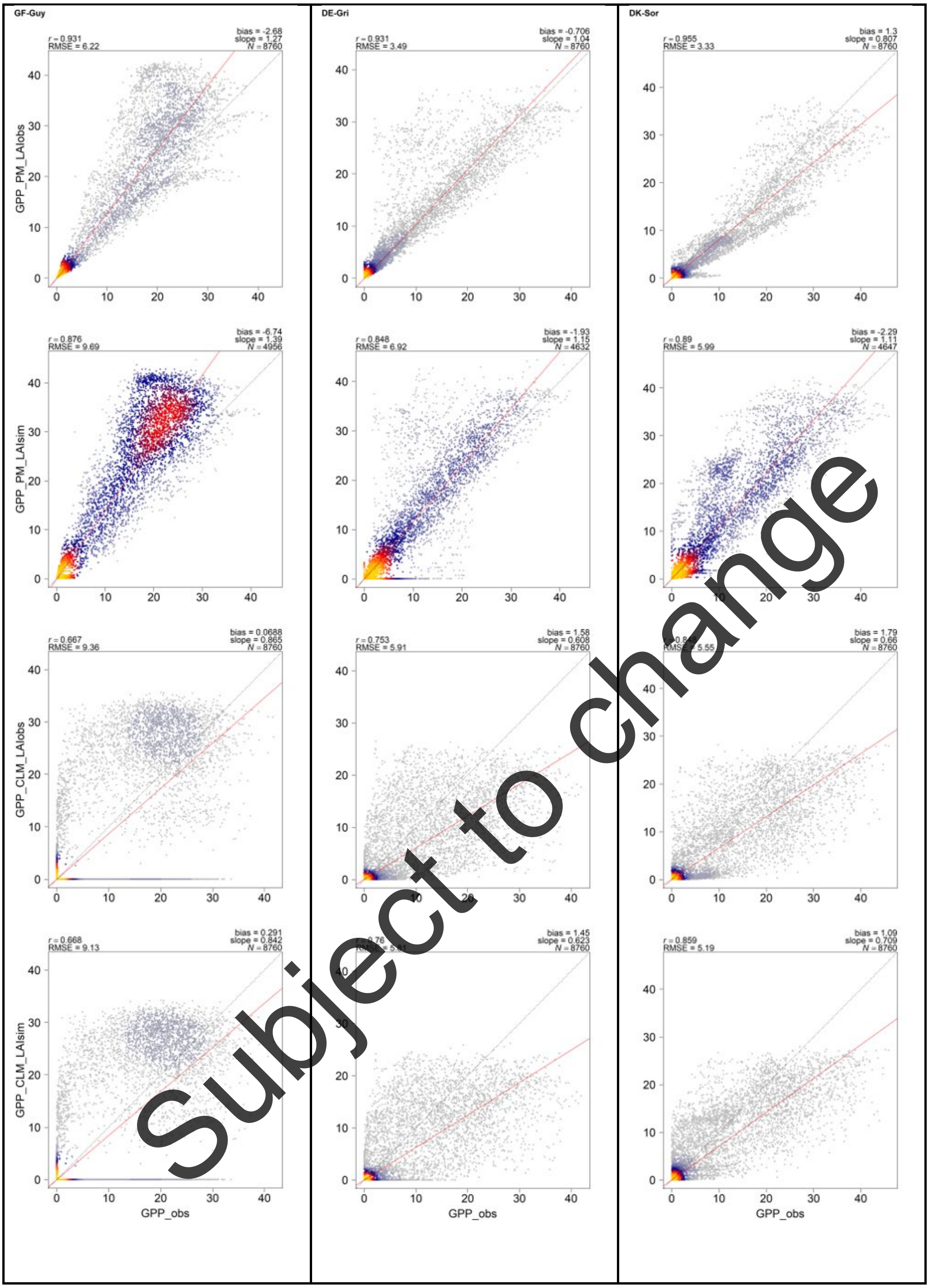

Figure 3: Heat map plot comparing simulated and observed sub-daily GPP across three sites. The scatter plot shows the GPP simulated by the P model and CLM using observed LAI (GPP_PM_LAIobs, GPP_CLM_LAIobs), simulated LAI (GPP_PM_LAIsim, GPP_CLM_LAIsim) compared to the flux-derived values (GPP_obs). The colour scale indicated data density, with red areas representing the highest concentration

of points. The 1:1 line represent the perfect agreement between observations and simulations. GPP is expressed in µmol CO2 m^{-2} s^{-1}

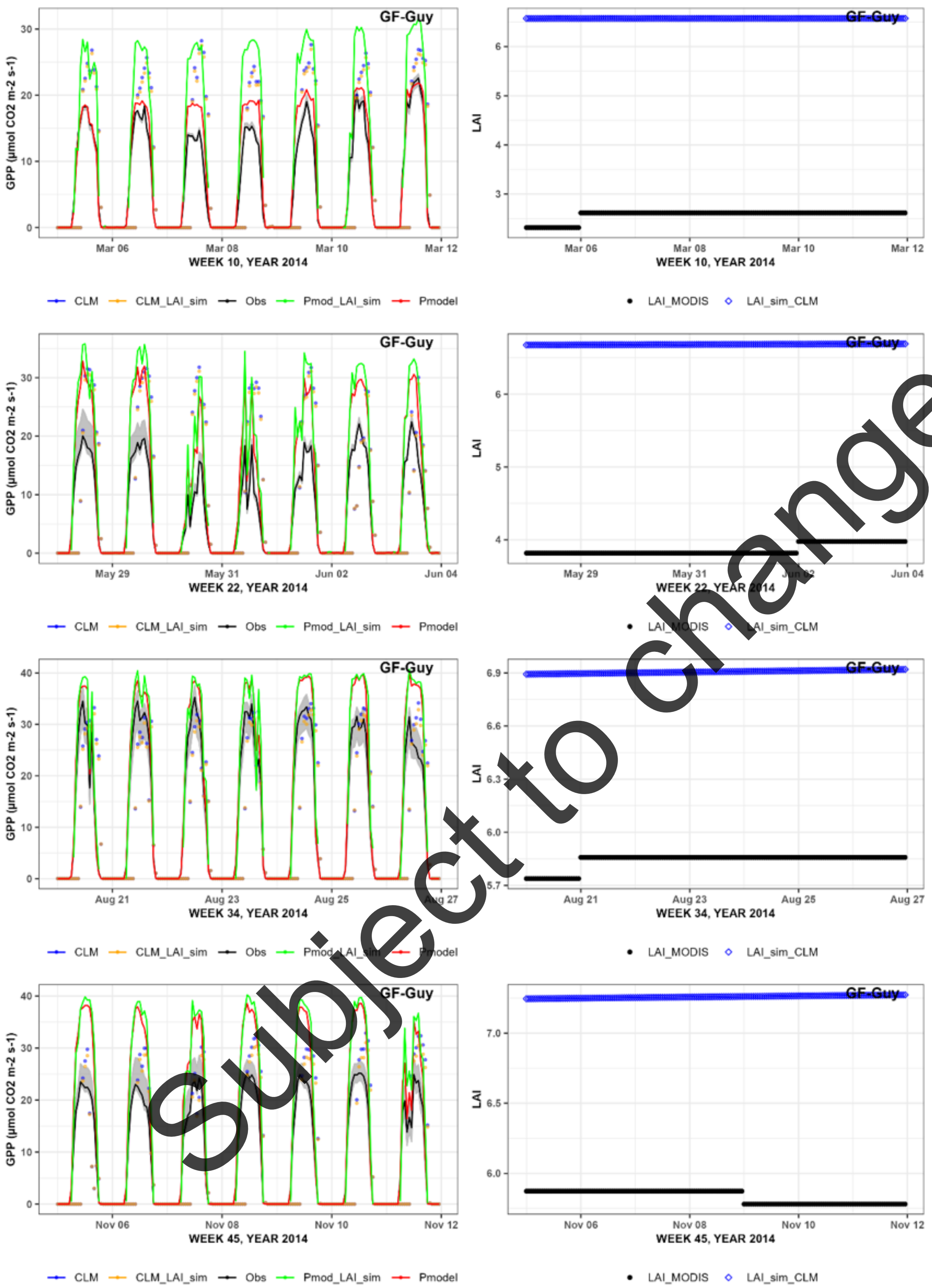

Figure 4: On the left, comparison of the GPP simulated by the P model and by CLM using the observed satellite LAI (Pmodel in red and CLM in blue) and the simulated LAI from CLM (Pmod_LAI_sim in green, CLM_LAI_sim in orange) and the GPP derived from eddy covariance flux-tower measurements, in 4

different weeks over 2014. On the right, comparison of simulated LAI (LAI_sim_CLM in blue) and observed LAI (LAI_MODIS in black) for the same 4 weeks in 2014. Sub-daily trends of GPP at GF-Guy, broadleaf evergreen tropical forest.

Figure 4 (continued) - Second site: DE-Gri, grassland.

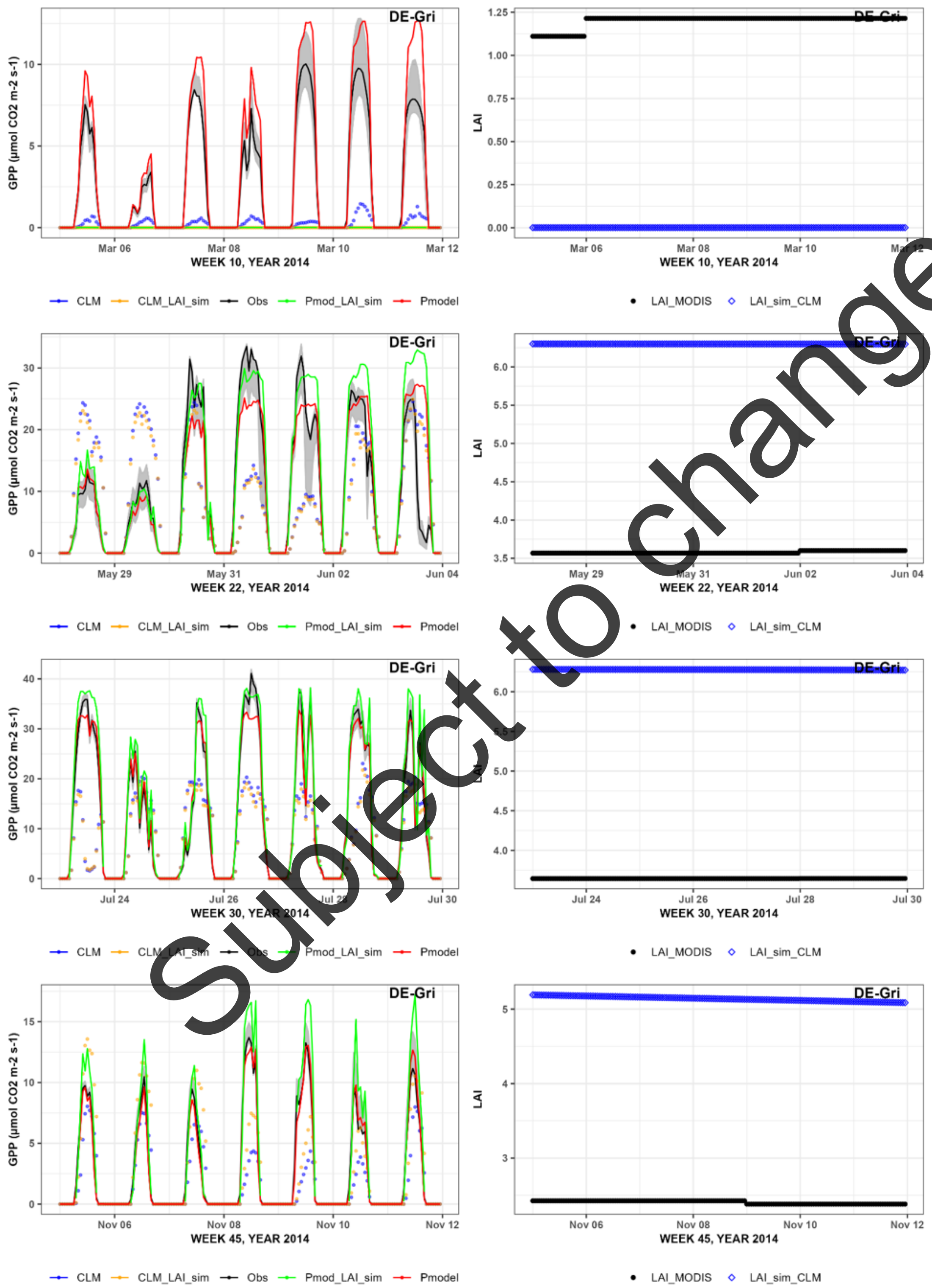

Figure 4 (continued) - Third site: DK-Sor, broadleaf deciduous temperate forest.

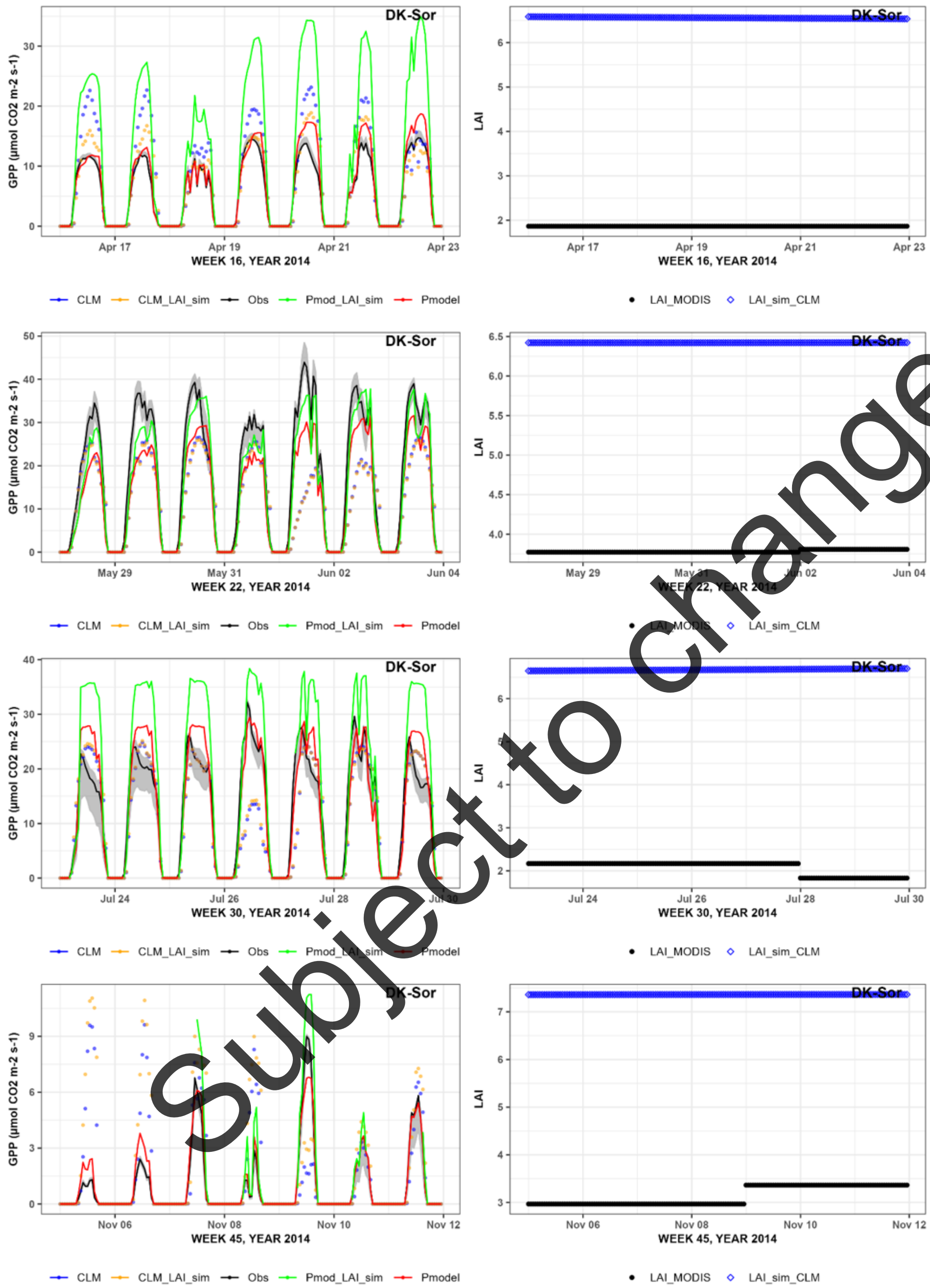

6.1.2. JULES implementation

Building on the site-level implementation and evaluation of the P model in JULES (PJULES: Gan et al., 2026), we have now extended testing to gridded, global-scale offline simulations. To evaluate the performance of PJULES, we compare carbon fluxes simulated by three JULES configurations, each using a different photosynthesis scheme: (1) Farquhar without acclimation (CTRL), (2) Farquhar with Kumarathunge acclimation (K-Acclim.), and (3) PJULES.

All three configurations are run at 0.5° spatial resolution with half-hourly timesteps over the period 1980–2016, using WFDEI meteorological reanalysis as atmospheric forcing and ESA-CCI LAI monthly climatology.

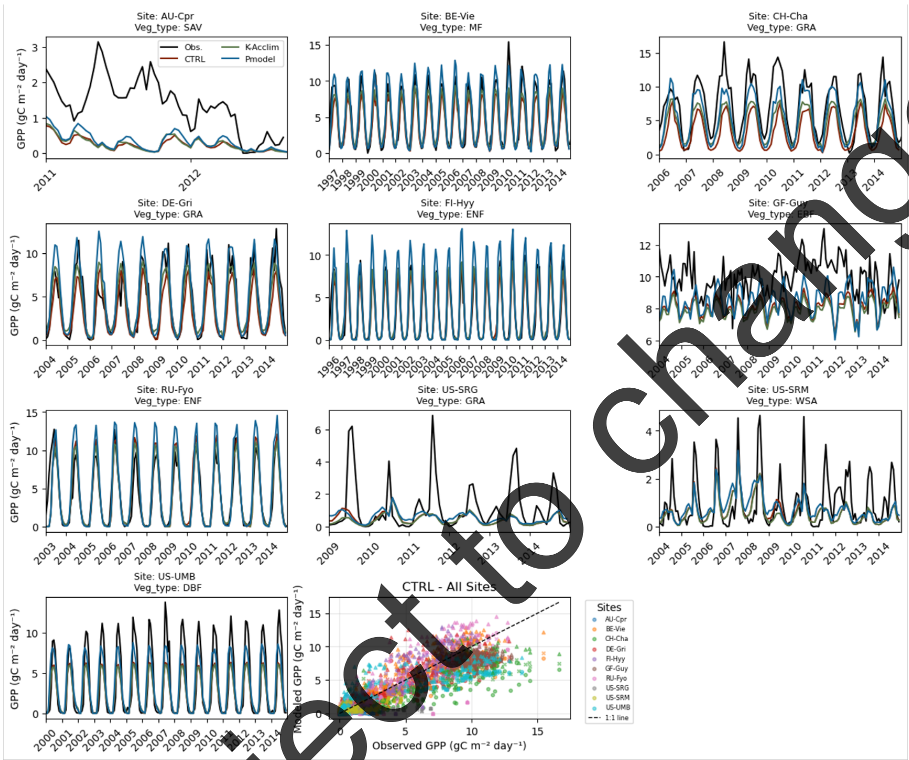

Figure 5: Comparison of three JULES photosynthesis schemes against the monthly means of GPP at the selected FLUXNET sites.

Figure 5 shows monthly GPP at FLUXNET sites extracted from the global simulation. The P model generally outperforms the other schemes across sites spanning a wide range of vegetation types. The two sites (AU-Cpr and US-SRG) where all three configurations show consistent underperformance are in semi-arid and arid regions, suggesting that arid-zone processes warrant specific attention.

Figure 6 presents the seasonal GPP budgets for each of the nine JULES plant functional types (PFTs). Across all seasons, the acclimation scheme produces higher fluxes than CTRL, with the P model yielding the largest fluxes overall, most notably for C3 grasses.

This pattern is consistent across seasons and points to meaningful differences in how the three schemes represent temperature and light responses of photosynthesis.

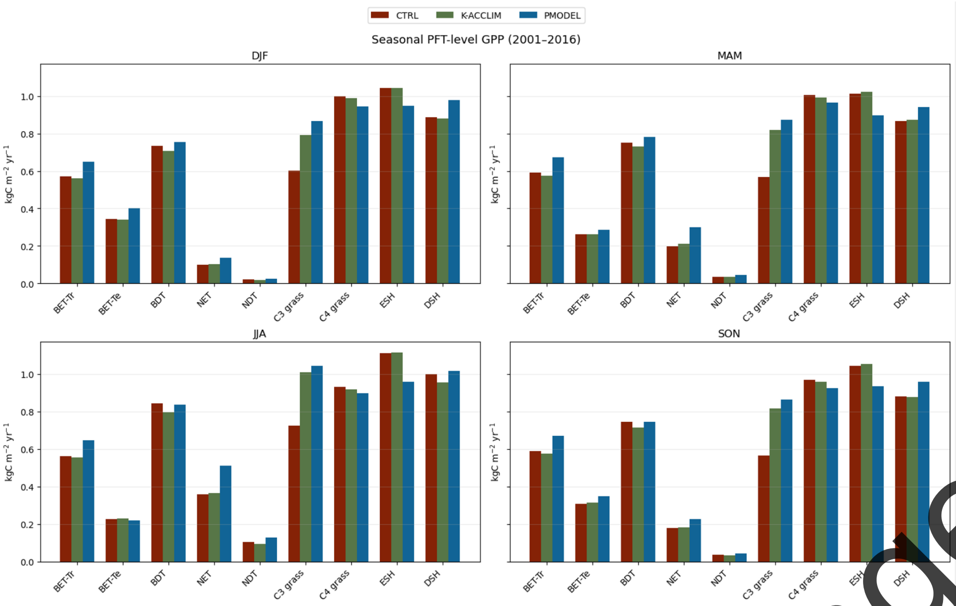

Figure 6: The seasonal GPP budgets simulated in the three JULES schemes for the 9 pft's of the model. PFT codes: BET=broadleaf evergreen tree (tropical/temperate), BDT=broadleaf deciduous tree, NET/NDT=needle-leaf evergreen/deciduous, and ESH/DSH=evergreen/deciduous shrub.

6.1.3. ecLand implementation

In order to explore the optimality theory within the ECMWF land surface model ecLand and evaluate its impact on the carbon fluxes, the sub-daily P model (Mengoli et al., 2022) is being implemented. To be integrated within ecLand a few points need to be addressed: The original P model relies on daily integration, therefore it needs adjustment to run at the sub-daily timestep to be integrated within ecLand . It was also originally implemented for C3 only plants without consideration of soil moisture stress. In this Task, the initial implementation of P model in ecLand is achieved and 1D-site simulations are performed. This was possible after the integration of the sub-daily adjustment in addition to the ongoing introduction of the C4-plants parameterisation.

Figures 7 shows the 10-day average GPP over 10 FLXUNET sites having different PFTs as simulated by ecLand using P model, and Farquhar parametrization compared to the sites' observations. All the ecLand simulations use the operational IFS monthly LAI climatology derived from the Copernicus Land Monitoring Service. Overall P model's GPP compares better with the observations except over dry sites such as the AU-Cpr Savannah site where possible improvement could be achieved once a proper soil moiXsture stress parameterisation is implemented.

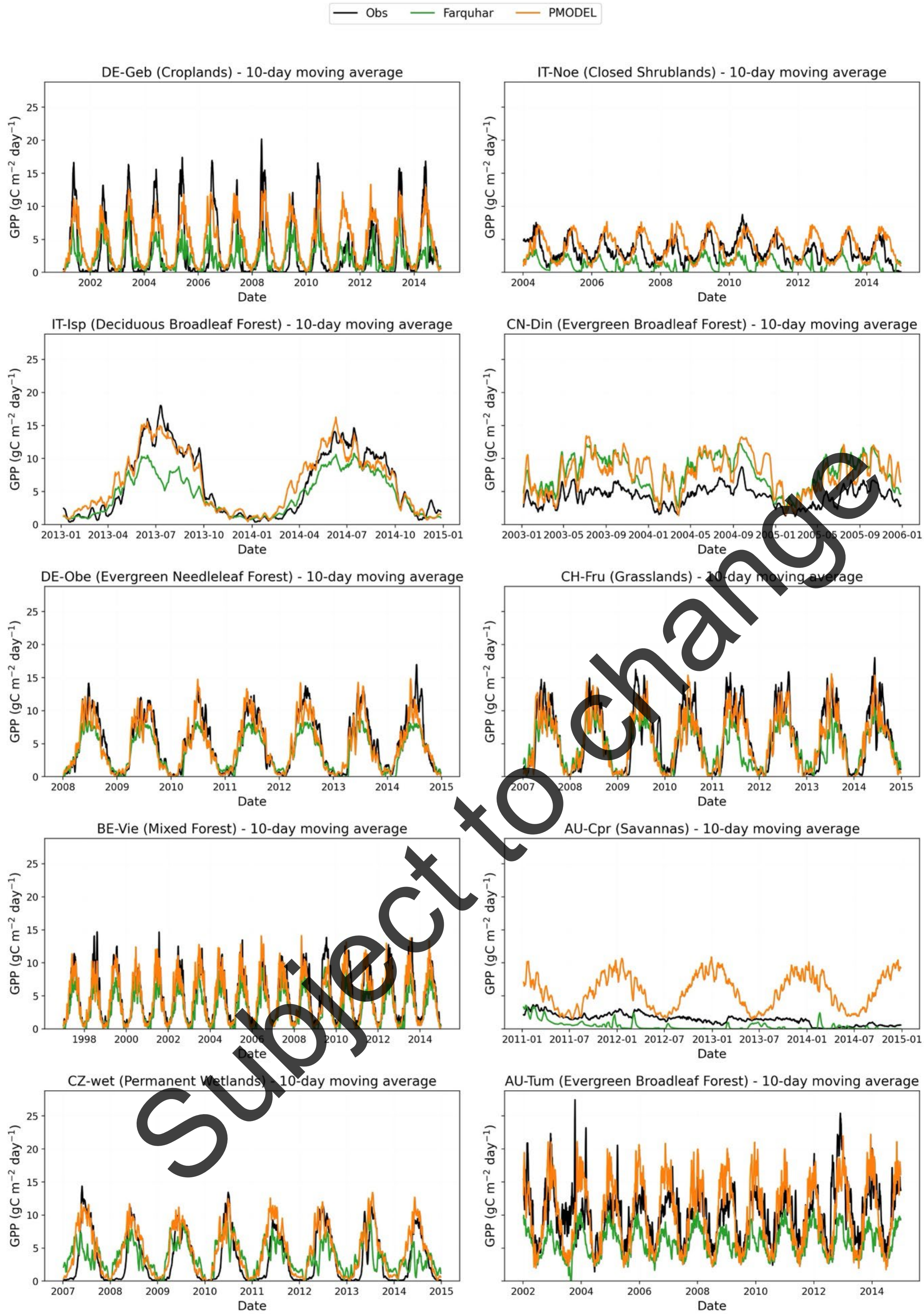

Figure 7: 10-day average GPP over 10 FLUXNET sites having different PFTs as simulated by ecLand using Pmodel (orange), and Farquhar (green) parametrization compared to the sites' observations (black).

6.2. Future developments

6.2.1. CLM implementation

At this stage, the implementation is not yet fully coupled to the CLM carbon-water framework, so the first actions are:

- Applying the water stress function of CLM to the integrated P model into CLM (PCLM).
- Implement the C4 schema for photosynthesis in PCLM, since it has been implemented and it is currently under testing in JULES.
- Evaluating the standard CLM photosynthesis scheme and the EEO-based photosynthesis scheme derived from the embedded P model within CLM (PCLM) at 142 sites, using the same meteorological forcings and satellite-observed LAI from MODIS and the Copernicus Global Land Service, the two global satellite products available within PLUMBER2. This evaluation aims at discovering systematic patterns where EEO performs better and where it does not, and understand if the water stress function used in CLM is enough to correct the known error in magnitude that the sub-daily P model shows in drylands.
- Possibly, in collaboration with the other consortium members, working on the improvement of model performance in arid sites, using different soil moisture stress functions, from empirical to optimality-based approaches. Designing and conducting experiments to investigate the impact of these different soil moisture functions within CLM and to compare the results with the P model implementations in ecLand and JULES, which rely on their own soil moisture stress formulations.
- Possibly working on the improvement of the LAI using an optimality-based approach.

Then, the CLM implementation will go from an offline diagnostic implementation to a prognostic investigation of the fully integrated sub-daily P model within CLM:

- Identification of the key land-surface processes linked to GPP to fully integrate the sub-daily P model into the CLM framework. Initial efforts focus on identifying how latent heat flux is represented and diagnosed within the CLM code structure.
- Development of the coupling interfaces between the embedded P model and the CLM framework. Investigation of the impact of the new implementation on evapotranspiration (ET).
- Intercomparison of implementation strategies and performance of the sub-daily P model across different LSMs.

6.2.2. JULES implementation

The preliminary global simulations have demonstrated that the P model produces encouraging results in JULES. The next stage of work will focus on implementing and testing other elements of EEO-theory in JULES.
The implementation and testing of the acclimation of leaf dark respiration is a future goal as well.

6.2.3. ecLand implementation

To improve its performance over arid and semi-arid regions, a soil moisture stress parameterisation will be introduced in the P model. Subsequently, the model will be implemented in 2D mode to allow global simulations driven by ERA5 atmospheric forcing and its evaluation under task T5.4.

7. ecLand implementation in EC-Earth4

7.1. Status of developments

Task 5.1 contains two sub-tasks related to the implementation of ecLand in EC-Earth4:

- Implementation of the improved ecLand version in the EC-Earth4 model, allowing for an improved representation of carbon fluxes between land and atmosphere in these ESMs at climate timescales.
- Incorporate the findings of T2.4 to replace the ecosystem respiration parameterisation of ecLand with an empirically-based scheme relying on carbon stocks derived from available ESA-CCI AGB data.

Since early beta releases of EC-Earth 4, ecLand has been technically available as the osmMASTER (or OSM; Offline Surface Model) within the OpenIFS 48R1 code, which has been modified for use in the EC-Earth4. However, the osmMASTER did not compile, thus BSC made some minor changes to the OpenIFS code to compile the osmMASTER program. We have made it possible to compile the osmMASTER in the IFS/NEMO bundle from ClimateDT for the TerraDT project. Within OpenIFS, there is no support for generating the required atmospheric forcings, nor for running the model. These important aspects have been made possible by adapting the scripts from the public ecLand model available at https://github.com/ecmwf-ifs/ecland. We implemented a number of missing features which are required to run ecLand within this project:

- Add basic support for reduced gaussian grid (ecland scripts only support regular lat/lon grid)
- Add support for time-varying vegetation (Land Cover and LAI)
- Scripts to run different ecLand model “flavours”: ecland-master from ecLand project and osmMASTER from EC-Earth4 and IFS-NEMO

- Add GSTATS performance statistics to identify bottlenecks
- Various improvements : Better management of forcing and output compression levels, MPI and OpenMP settings, generation of forcings for different grids and regions; compilation scripts; flexible interface to load environment for different machines, model flavours and system modules; caching of raw ERA5 forcings and initial conditions; avoid using CDS API whenever possible to use local boundary conditions; slurm submission scripts for forcing creation and running the model; capability to run several months/years in sequence; preparing for use of the Autosubmit workflow manager

No tangible progress has been made on the second sub-task, however we noted some inconsistencies in the CONCERTO Grant Agreement. The work in T2.4 will produce an annual NPP parameterisation, but ecLand requires a daily or sub/daily parameterisation, therefore the findings of T2.4 cannot be used to replace the ecosystem respiration parameterisation of ecLand. We are investigating alternative solutions to make progress on this topic.

7.2. Future developments

The following technical developments will be made in the next few months:

- Full support of gaussian grid (outputs, etc,)
- Workflow to generate land initial conditions for the seasonal forecast demonstrators in WP6
- Integration of time-varying LC and LAI datasets from WP2
- Implementation of several improvements to ecLand by ECMWF, such as prognostic LAI and P model
- Investigate solutions to improve carbon fluxes at seasonal timescales and replace ecosystem respiration
- Add support for forcings to be used in the offline simulations planned in T5.4
- Include full support for ecLand in the EC-Earth4 model framework

8. References

Bertagni, M. B., Regnier, P., Yan, Y. and Porporato, A., 2024. 'A dimensionless framework for the partitioning of fluvial inorganic carbon', *Geophysical Research Letters*, 51, e2024GL111310. https://doi.org/10.1029/2024GL111310

Boussetta, S., Balsamo, G., Arduini, G., Choulga, M., Albergel, C., Beljaars, A., Wedi, N., Lawrence, H., de Rosnay, P., Muñoz-Sabater, J. and Agustí-Panareda, A., 2021. 'ECLand: The ECMWF Land Surface Modelling System', *Atmosphere*, 12(6), p. 723. https://doi.org/10.3390/atmos12060723

Camporeale, C., & Latella, M. (2025). Stochastic dynamics of coastal dune vegetation. *Journal of Geophysical Research: Earth Surface*, 130, e2025JF008610. https://doi.org/10.1029/2025JF008610

Calvet, J.-C. and Soussana, J.-F., 2001. 'Modelling CO2-enrichment effects using an interactive vegetation SVAT scheme', *Agricultural and Forest Meteorology*, 108(2), pp. 129–152. https://doi.org/10.1016/S0168-1923(01)00235-0

Gan, W., Alizadeh, N., Best, M., Vidale, P. L., Prentice, I. C. and Harrison, S. P., 2026. 'An eco-evolutionary optimality model explains the acclimated temperature response of photosynthesis', *New Phytologist*, 250, pp. 2884–2899. https://doi.org/10.1111/nph.71062

Gibelin, A.-L., Calvet, J.-C., Roujean, J.-L., Jarlan, L. and Los, S. O., 2006. 'Ability of the land surface model ISBA-A-gs to simulate leaf area index at the global scale: Comparison with satellites products', *Journal of Geophysical Research: Atmospheres*, 111(D18), pp. 1–17. https://doi.org/10.1029/2005JD006691

Han, Q.; Belcore, E.; Morra di Cella, U.; Salerno, L.; Camporeale, C. Detection of Large Woody Debris in Braided-Rivers RGB-UAV Dataset: A Comparative Study. *Remote Sens.* **2026**, *18*, 900. https://doi.org/10.3390/rs18060900

Mengoli, G., Agustí-Panareda, A., Boussetta, S., Harrison, S. P., Trotta, C. and Prentice, I. C., 2022. 'Ecosystem photosynthesis in land-surface models: A first-principles approach incorporating acclimation', *Journal of Advances in Modeling Earth Systems*, 14(1). https://doi.org/10.1029/2021MS002767

Stocker, B. D., Wang, H., Smith, N. G., Harrison, S. P., Keenan, T. F., Sandoval, D., Davis, T. and Prentice, I. C., 2020. 'P-model v1.0: an optimality-based light use efficiency model for simulating ecosystem gross primary production', *Geoscientific Model Development*, 13(3), pp. 1545–1581. https://doi.org/10.5194/gmd-13-1545-2020

Vendruscolo, M., Salerno, L., Camporeale, C. and Ridolfi, L., 2025. 'Network-driven dispersion in transport phenomena', *Physical Review E*, 111, 054313. https://doi.org/10.1103/PhysRevE.111.054313